Carbohydrate Polymers 102 (2014) 269–277

Contents lists available at ScienceDirect

Carbohydrate Polymers

journal homepage: www.elsevier.com/locate/carbpol

Structural characterization of inclusion complexes between cyanidin-3-*O*-glucoside and β-cyclodextrin

Ana Fernandes[a], Galya Ivanova[b], Natércia F. Brás[b], Nuno Mateus[a], Maria J. Ramos[b], Maria Rangel[c], Victor de Freitas[a,*]

[a] Centro de Investigação em Química (CIQ), Departamento de Química e Bioquímica, Faculdade de Ciências, Universidade do Porto, Rua do Campo Alegre, 687, 4169-007 Porto, Portugal
[b] REQUIMTE, Departamento de Química e Bioquímica, Faculdade de Ciências, Universidade do Porto, Rua do Campo Alegre, s/n, 4169-007 Porto, Portugal
[c] REQUIMTE, Instituto de Ciências Biomédicas de Abel Salazar, Universidade do Porto, Rua Jorge Viterbo Ferreira, 228, 4050-313 Porto, Portugal

ARTICLE INFO

Article history:
Received 7 June 2013
Received in revised form 6 November 2013
Accepted 26 November 2013
Available online 4 December 2013

Keywords:
Anthocyanins
β-Cyclodextrin
DOSY
Molecular Dynamics simulations
NMR
ROESY

ABSTRACT

Inclusion complex formation between the multiple equilibrium forms of cyanidin-3-*O*-glucoside (cy3glc) and β-cyclodextrin (β-CD) was investigated using a combined approach of NMR spectroscopy and Molecular Dynamics simulation. Diffusion ordered NMR spectroscopy (DOSY) and study of nuclear Overhauser effects (NOE) were used to determine the selective intermolecular interactions and structure of these complexes in aqueous solution.

The observed chemical shift displacements of resonance signals of protons from the interior of β-CD cavity and protons belonging to the hemiketal (**B**) and *cis*-chalcone forms (**Cc**), the diffusion measurements using DOSY and the NOE studies have anticipated the formation of an inclusion complex between these two forms and β-CD. The analysis of the NMR spectral data has shown no evidence of internal interaction between β-CD and the flavylium cation (**AH**$^+$) or *trans*-chalcone (**Ct**) forms of cy3glc.

The hemiketal formed a 1:1 inclusion complex with β-cyclodextrin in which the pyranic C ring is deeply included inside the β-CD cavity while B ring lies on the plane of the wider rim of β-CD. The structure of the complexes was also clarified through a theoretical approach by Molecular Dynamics simulation.

1. Introduction

Cyclodextrins (CD) are cyclic oligosaccharides consisting of six or more (1→4)-α-D-glucopyranose units, possessing the remarkable ability of forming inclusion complexes with a variety of organic molecules (Scheme 1) (Rymdén, Carlfors, & Stilbs, 1983; Thaning et al., 2008). Due to their unique structural features, these molecules are invaluable in a variety of industrial applications namely in the Food Industry, where they have been used for controlling flavor release, masking odors and tastes, stabilizing emulsions, controlling or masking color, and protecting ingredients from oxidation and from thermal decomposition (Del Valle, 2004; Szejtli, 2003).

In recent years, replacing synthetic dyes by natural colorants has become a major issue for the Food Industry since the use of synthetic additives is becoming less popular among the consumers as they easily associate these colorants to toxic issues.

Anthocyanins are potentially very interesting as natural food colorants due to their ability to impart vibrant colors. These polyphenolic compounds provide colors ranging from salmon-pink to red and violet, they are water-soluble pigments which simplifies their incorporation in aqueous food systems and do not pose any particular problems in terms of food safety (Torskangerpoll & Andersen, 2005). On the contrary, these compounds are antioxidant and were described to have some putative beneficial health effects (Clifford, 2000; He & Giusti, 2010).

However, the application of anthocyanins as food colorants requires improvement of their chemical stability since they are very unstable and susceptible to be transformed in food matrices during storage (Ersus & Yurdagel, 2007). The fact that anthocyanins co-exist in aqueous solution in a complex network of equilibrium species depending on pH is an important factor related to the color displayed by these compounds. In very acidic aqueous solutions, the red flavylium cation (**AH**$^+$) is predominant. As pH increases, water addition on flavylium cation gives rise to the colorless hemiketal (**B**). This specie is in fast equilibrium with some yellow *cis*-chalcone (**Cc**). Finally, the slowest process is the *cis-trans* isomerization to lead to a small mole fraction of yellow *trans*-chalcone at equilibrium (**Ct**). Concurrently, deprotonation of the flavylium cation also occurs, leading to blue-purple quinoidal bases (**A**) (Brouillard & Delaporte, 1977; Brouillard & Dubois, 1977; Brouillard & Lang, 1990) (Scheme 1). For anthocyanins, the quinoidal bases are

* Corresponding author. Tel.: +351 220402558; fax: +351 220402659.
E-mail address: vfreitas@fc.up.pt (V. de Freitas).

0144-8617/$ – see front matter © 2013 Elsevier Ltd. All rights reserved.
http://dx.doi.org/10.1016/j.carbpol.2013.11.037

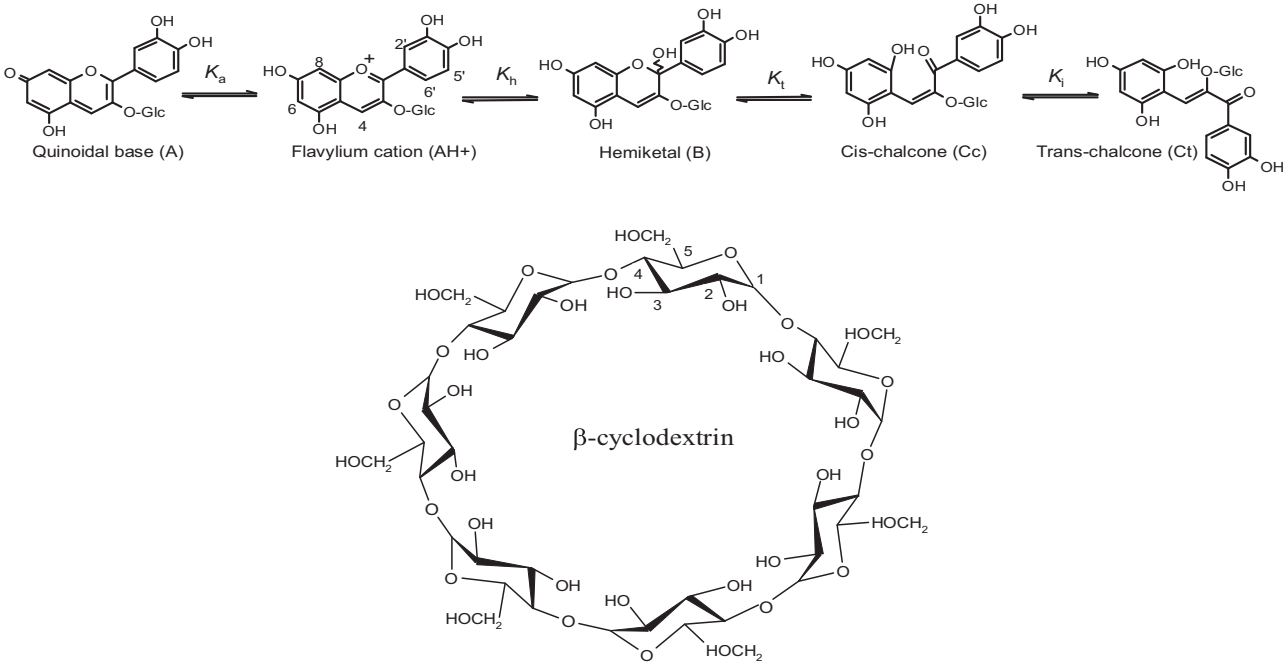

Scheme 1. Network of the equilibrium forms of cyanidin-3-*O*-glucoside at different pH values and chemical structure of β-cyclodextrin.

not the most stable specie at the equilibrium and they tend to disappear to form the most stable hemiketal (**B**) form (Pina, Melo, Laia, Parola, & Lima, 2012).

The formation of inclusion complexes between cyclodextrins and anthocyanins was found to improve the anthocyanin stability and prevent losses during storage (Chandra, Nair, & Iezzoni, 1993; Howard, Brownmiller, Prior, & Mauromoustakos, 2013; Lewis, Walker, & Lancaster, 1995; Mourtzinos et al., 2008; Tamura, Takada, Yamagami, & Shiomi, 1998). However, in several studies an anti-copigmentation effect was described, resulting from the better inclusion of the colorless forms into the cyclodextrin cavity (Dangles, Wigand, & Brouillard, 1992; Lewis et al., 1995; Yamada, Komiya, & Akaki, 1980). Some preliminary kinetic results have also demonstrated the preferable inclusion of these forms, established on the increase of the hydration constant (K_h) (Fernandes, Sousa, Azevedo, Mateus, & de Freitas, 2013) and on the isomerization observed rate constant (k_{obs}) (Dangles, Stoeckel, Wigand, & Brouillard, 1992; Dangles, Wigand, et al., 1992).

Therefore, a correct knowledge of the factors that govern anthocyanin's color stability seems to be decisive in terms of a putative application in food matrices. The aim of the present work was to distinguish the different anthocyanin (cy3glc) colorless forms by their tendency for associating with β-cyclodextrin in aqueous solution. For this purpose, a combination of NMR experiments (ROESY and DOSY) and a theoretical approach has been undertaken.

2. Experimental part

2.1. Materials

β-Cyclodextrin (β-CD) and deuterium oxide (D_2O) (99.9%) were purchased from Sigma–Aldrich® (Madrid, Spain). Cyanidin-3-*O*-glucoside (cy3glc) was extracted and purified in the laboratory from blackberries (*Rubus fruticosus*) by semipreparative HPLC with C_{18} reversed phase column, as described elsewhere (Azevedo et al., 2010).

2.2. Sample preparation

Solutions of cyanidin-3-*O*-glucoside at different concentrations (8.6 mM, 5.2 mM, 2.7 mM, 2.1 mM and 1.4 mM) and β-cyclodextrin (8.6 mM) were prepared in 99.9% D_2O at room temperature and pD was adjusted to 3.9 by the addition of NaOD (Popov, Rönkkömäki, & Lajunen, 2006). For the study of the inclusion complexes formation 1.4 mM of cyanidin-3-*O*-glucoside was dissolved in 99.9% D_2O and appropriate amounts of β-cyclodextrin were added (1.2 mM; 1.4 mM; 2.2 mM; 3.4 mM and 4.5 mM). pD was also adjusted to 3.9. Samples were allowed to equilibrate for at least 8 h before the NMR study.

2.3. Uv–vis absorption spectra

Absorption spectra of cyanidin-3-*O*-glucoside solution (1.4 mM) and absorption spectra of samples of cyanidin-3-*O*-glucoside and β-cyclodextrin at different concentrations were obtained in an UV–vis spectrophotometer (Thermo Scientific Evolution Array UV-vis spectrophotometer) fitted with a thermostated 1.0 cm path length cuvette device at 25 °C.

2.4. NMR spectroscopy

All NMR experiments were recorded on a Bruker Avance III 600 HD spectrometer, operating at 600.13 MHz for protons and 150.92 MHz for carbon, equipped with 5 mm CryoProbe Prodigy and pulse gradient units, capable of producing magnetic field pulsed gradients in the *z*-direction of 50 G/cm. The NMR measurements have been done with standard BRUKER pulse sequences, in deuterium oxide (D_2O), at 300 K and at pD 3.9. ^1H NMR experiments were performed with water suppression using excitation sculpting with gradients (Hwang & Shaka, 1995), acquisition time 1.36 s, relaxation delay 2 s, 128 or 256 transients of a spectral width of 10,000 Hz were collected into 32 K time domain points. Typical measuring conditions for the $^1H/^1H$ and 2D spectra (COSY, TOCSY, ROESY, NOESY) recorded in phase sensitive mode and with water suppression were: relaxation delay 2 s, 64–128 scans, a total 2 K

data points in *F*2 and 256 data points in *F*1 over a spectral width of 10,000 Hz. TOCSY spectra were recorded MLEV-17 sequence with a mixing time of 80 ms. ROESY experiments were carried out using a mixing time of 100, 200, 400, 500, 700 and 800 ms in the phase-sensitive mode. 2D 1H/13C HSQC and HMBC experiments were carried out with a spectral width of *ca* 10,000 Hz for 1H and 32,000 Hz for 13C, relaxation delay 1.5 s, Fourier transform (FT) size 2 K × 1 K.

Proton registered diffusion-ordered NMR (^{1}H DOSY) experiments were acquired using the bipolar longitudinal eddy current delay (BPPLED – Bipolar Pulsed Field Gradient Longitudinal Eddy Delay) pulse sequence (Wu, Chen, & Johnson, 1995). The experimental conditions (5 mm NMR tubes, amount of the solute and solvent, a temperature of 300 K, no sample rotation and high air flow of 535 L/h to avoid convections in the samples) for all DOSY experiments were kept constant. Before the NMR experiments, the temperature was equilibrated and maintained at 300 K, as measured using the spectrometer thermocouple system. Typically, in each experiment a number of 16 spectra of 32 K data points and 128 or 256 scans were collected, with values for the duration of the magnetic field pulse gradients (δ) of 2.4 ms, diffusion times (Δ) of 120 ms and an eddy current delay set to 5 ms. The pulse gradient (g) was incremented from 2 to 98% of the maximum gradient strength in a linear ramp. The spectra were processed with the Bruker Topspin software package (version 3.2). The diffusion coefficients (*D*) were obtained by measuring the signal intensity of characteristic resonances of the species presented in the samples studied and were all scaled to the absolute *D* value obtained for acetone (0.001 M; 1.69×10^{-9} m^2 s^{-1}, calculated standard deviation of 1.15×10^{-3}) used as an internal reference.

2.5. Molecular Dynamics simulation

The initial structure of β-cyclodextrin (β-CD) was obtained from its complex with cyclo/maltodextrin-binding protein (pdb id: 2ZYN at 1.7 Å resolution) (Matsumoto et al., 2009) retrieved from the protein databank. Given the absence of cyanidin-3-*O*-glucoside (cy3glc) structure in this database, the initial geometry of this compound was built with the GaussView software (Gaussian Inc., Pittsburgh, PA). To calculate the optimized geometries and electronic properties for the subsequent parameterization of this compound, the Gaussian 09 suite of programs (Frisch et al., 2009) was used to perform restricted Hartree–Fock calculations (RHF), with the 6-31G(d) basis set. Atomic charges were further recalculated using RESP algorithm (Bayly, Cieplak, Cornell, & Kollman, 1993). This methodology was chosen for its consistency with that adopted for the parameterization process in AMBER 10.0 simulation package (Case et al., 2008). The geometry optimizations and a Molecular Dynamics (MD) simulation on cy3glc:β-CD complex were performed with the parameterization adopted in AMBER 10.0, using the GAFF force field, the general Amber force field for small organic molecules, and the Glycam2004 force field (Glycam-04 parameters) for carbohydrates (Basma, Sundara, Calgan, Vernali, & Woods, 2001; Kirschner & Woods, 2001a, 2001b). In this simulation, an explicit solvation model with pre-equilibrated TIP3P water molecules was used, filling a truncated octahedral box with a minimum distance of 12 Å between the box faces and any atom of the cy3glc:β-CD complex. The size of this system was 6004 atoms. The complex geometry was minimized in two stages: first both compounds were kept fixed and only the position of the water molecules was minimized. Afterwards the full system was minimized. Subsequently, an MD simulation of 100 ps at constant volume and temperature, and considering periodic boundaries conditions was run, followed by 30 ns of MD simulation with NPT ensemble, in which Langevin dynamics was used (collision frequency of 1.0 ps^{-1}) to control the temperature at 303.15 K (Izaguirre, Catarello, Wozniak, & Skeel, 2001). These simulations were carried out using the Sander module, the bond lengths involving hydrogen atoms were constrained using the SHAKE algorithm, and the equations of motion were integrated with a 2 fs time step using the Verlet leapfrog algorithm (Ryckaert, Ciccotti, & Berendsen, 1977). The Particle-Mesh Ewald (PME) method (Essmann et al., 1995) was used to include the long-range interactions, and the nonbonded interactions were truncated with a 10 Å cutoff. The MD trajectory was saved every 2 ps and the MD results were analyzed with the PTRAJ module of AMBER 10.0 (Case et al., 2008).

3. Results and discussion

The ability of cyclodextrins to form an inclusion complex with a guest molecule is a function of two key factors. The first concerns the steric requirements and depends on the relative size of the cyclodextrin to the size and to the physical–chemical properties of the molecule to include. The second critical requirement corresponds to the thermodynamic interactions between the different components of the system (Del Valle, 2004). For a complex to be formed there must be a favorable net energetic driving force that pulls the guest into the cyclodextrins and a variety of noncovalent forces such as van der Waals forces, hydrogen bonds and other forces are responsible for the formation of a stable complex (Bourvellec, 2003).

In the present work, the ability for inclusion complex formation between the different equilibrium forms of cy3glc and β-CD in aqueous solution and the structure of these inclusion complexes were studied by NMR spectroscopy and theoretical calculations. pD 3.9 was selected to perform this study since at this pD value approximately 75% of the anthocyanin corresponds to the hemiketal form with the remaining 25% corresponding to the flavylium cation, to the *cis* and *trans*-chalcone and to the quinoidal base form (Pina et al., 2012).

3.1. NMR spectral characterization of cy3glc

The detailed knowledge of the structural and spectral characteristics of anthocyanins is of primary significance prior to the investigation of the molecular structure of inclusion complexes with β-cyclodextrin. It is well known that anthocyanins can coexist in aqueous solution in equilibrium between five species depending on pH (Scheme 1). Additionally, the relative species population is affected by the possible self-association of anthocyanins as a result of the vertical stacking caused by hydrophobic interaction between aromatic rings (Dangles, Stoeckel, et al., 1992; Hoshino, Matsumoto, Harada, & Goto, 1982; Houbiers, Lima, Maçanita, & Santos, 1998; Leydet et al., 2012).

Therefore, a preliminary NMR spectral characterization of cy3glc in aqueous solution, at pD 3.9 and different concentrations was performed. The assignment of the resonance signals in ^{1}H NMR spectra of anthocyanin was based on the analysis of one and two dimensional (COSY, TOCSY, HSQC, HMBC) NMR spectra. The NMR data are consistent with the data already published (Houbiers et al., 1998; Jordheim, Fossen, & Andersen, 2006; Santos et al., 1993) and the assignments of the chemical shifts and coupling constants of protons H2′, H6′, H5′ and H4 in the different equilibrium forms are presented in Table 1. The resonance signals of protons H6 and H8 in the A ring disappeared from the spectrum a few hours after sample preparation due to protons exchange with deuterium (Houbiers et al., 1998; Ishizu, Hirata, Yamamoto, & Harano, 2006). The hemiketal can be easily identified not only because it is the major specie at this pH value but also because of the existence of twin peaks related to the presence of the two epimers (*R*/*S*) on

Table 1
^1H (600.13 MHz) NMR data (proton chemical shift (ppm), multiplicity and spin-spin coupling constant (Hz)) and diffusion coefficient (D) for the flavylium cation, hemiketal, *cis*-chalcone and *trans*-chalcone equilibrium forms of 8.6 mM and 1.4 mM cyanidin-3-*O*-glucoside solutions in D_2O at pD 3.9.

	Cyanidin-3-*O*-glucoside							
	Flavylium (AH^+)		Hemiketal (B)		*Cis*-chalcone (Cc)		*Trans*-chalcone (Ct)	
	8.6 mM	*1.4 mM*	*8.6 mM*	*1.4 mM*	*8.6 mM*	*1.4 mM*	*8.6 mM*	*1.4 mM*
Aglicone								
$H_{2'}$	7.23 *s*	7.67 *s*	7.08 *d*/7.04 *d (2.2)*	7.09 *d*/7.06 *d (2.2)*	–	7.23 *d (2.0)*	–	7.39 *d (2.2)*
$H_{5'}$	6.50 *d (8.2)*	6.84	6.86 *d (8.6)*	6.88 *d (8.6)*	–	6.70 *d (8.6)*	–	6.95 *d (8.5)*
$H_{6'}$	7.44 *d (8.2)*	7.79	6.99 *dd*/6.95 *dd (8.6; 2.2)*	7.02 *dd*/6.99 *dd (8.4; 2.2)*	–	7.21 *dd (8.0; 2.0)*	–	7.42 *dd (8.6; 2.0)*
H_4	8.21 *s*	8.60 *s*	6.33 *s*/6.32 *s*	6.41 *s*/6.38 *s*	–	6.54 *s*	–	6.73 *s*
$D \times 10^{-10}$ ($m^2 s^{-1}$)	3.24	4.20	5.34	5.55	–	5.50	–	5.59

s, singlet; *d*, doublet; *dd*, double doublet.

Fig. 1. ^1H NMR spectra of cyanidin-3-*O*-glucoside in D_2O at pD 3.9 as a function of concentration (8.6 mM (A); 5.2 mM (B); 2.7 mM (C); 2.1 mM (D), 1.4 mM (E)).

carbon 2 (C2). The *cis*- and *trans*-chalcones usually appear at low concentrations (Leydet et al., 2012).

From the analysis of the ^1H NMR spectra performed at decreasing concentrations (8.6–1.4 mM) a systematically downfield shift of the resonance signals of the flavilyum and a significant accumulation of hemiketal form and the appearance of weak signal from *cis*- and *trans*-chalcone were observed (Fig. 1). The self-association of anthocyanins is a well-known phenomenon taking place with the flavylium cation as well as with the quinoidal base. Cross aggregation involving flavylium cation and *trans*-chalcone was also described (Leydet et al., 2012) and in this work, the self-association of the flavylium cation was perceived through the downfield shift with the anthocyanin concentration decrease.

The detected changes in ^1H NMR spectra were attributed to the disruption of the self-aggregate complexes of anthocyanins and more specifically of the flavilyum with the decrease of cy3glc concentration. Perceptibly, the disruption of the aggregation phenomenon affects the equilibrium between the four species in the aqueous solution resulting in a significant increase of the **B** form and appearance of **Cc** and **Ct** forms at solution concentration under 1.4 mM. The concentration dependence of self-association of cy3glc species was additionally estimated on the basis of the alteration of their self-diffusion coefficients as measured by DOSY experiments. The diffusion coefficients measured for the different species presented in the solution of cy3glc at 9 and 1.4 mM are presented in Table 1. It is possible to observe that the D value for the flavylium cation form was significantly affected by the concentration as a result of its self-aggregation. Micellarization process is a well-known phenomenon taking place in procyanidins (Cala et al., 2012; Pianet et al., 2008) and similarly to these polyphenolic compounds, by plotting the flavylium cation D value against the inverse anthocyanin concentration we could obtain an approximated cac, critical aggregation concentrations ($\sim$1 g L^{-1} in supplementary materials). However to ensure that the flavylium cation behaves such as procyanidins undergoing a micellarization process, more anthocyanin concentration should be tested.

3.2. NMR analysis and stoichiometry of the inclusion complex cy3glc:β-CD

Evaluation of the changes in chemical shifts of β-cyclodextrin upon complexation provided the first information about the host–guest interaction allowing the determination of the stoichiometry of the inclusion complexes. The reasoning is based on

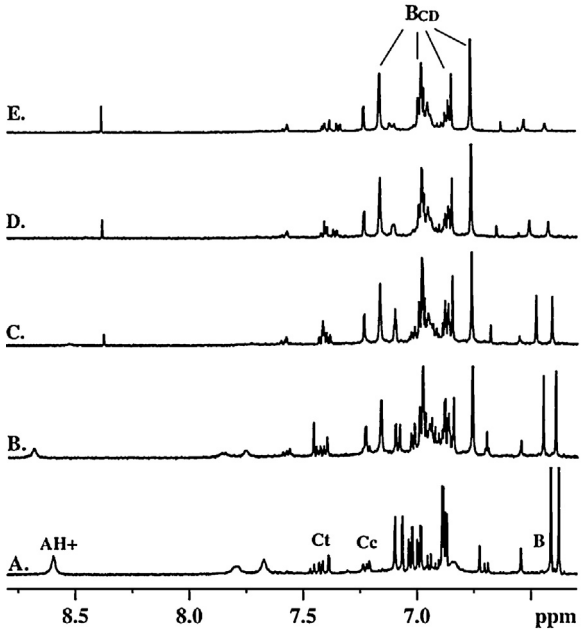

Fig. 2. ^{1}H NMR spectra of 1.4 mM cyanidin-3-*O*-glucoside solution in D_2O at pD 3.9 (**A**) and ^{1}H NMR spectra of cyanidin-3-*O*-glucoside with increasing ratios of β-CD after reaching equilibrium (1:0 (A); 1:0.8 (B); 1:1.6 (C); 1:2.4 (D); 1:3.2 (E)).

the expectation that if the guest molecule is imbedded in the CD cavity, the screening environment should be sensed by magnetic nuclei inside the β-CD cavity (H3 and H5) but not by outside protons (H1, H2 and H4) (Polyakov, Leshina, Hand, Petrenko, & Kispert, 2004).

In order to minimize the effect of the self-aggregation of the anthocyanin, the lowest solution concentration (1.4 mM) was selected to perform the subsequent NMR study of the interaction between cy3glc and β-CD and for structural characterization of cy3glc:β-CD complex (Fig. 2). ^{1}H NMR spectra with high resolution were recorded for cy3glc:β-CD in D_2O at pD 3.9. The spectra are dominated by the intense resonance signals of β-CD and upfield shifts of the resonance signals of H3 and H5 β-CD's protons were detected. This behavior may result mainly from the magnetic anisotropic shielding by the aromatic rings in cy3glc molecules, included within the cavity of β-CD (Ishizu et al., 2006; Ishizu, Kajitani, Tsutsumi, Yamamoto, & Harano, 2008). Only minor alterations in the chemical shift of protons H1, H2 and H4 which lie on the outer surface of the cavity was observed.

In the ^{1}H NMR spectra of cy3glc:β-CD, signals belonging to the protons of **AH$^+$**, **B**, **Cc** and **Ct** forms of cy3glc were clearly observed. Additionally, it was found that the addition of β-CD to the aqueous solution of cy3glc immediately induced the appearance of new set of resonance signals identified as $\mathbf{B_{CD}}$ (Fig. 2B–E). The intensity of these signals increased while the intensity of the resonance signals of the **B** form decreased with time. On the basis of 1D and 2D (TOCSY, HMBC) NMR analysis, these new signals were attributed to the hemiketal anthocyanin form complexed with β-CD ($\mathbf{B}_{CD}$). Well defined long range correlations were observed in the ^{1}H/^{13}C HMBC spectra between characteristic signals of the $\mathbf{B_{CD}}$, such as between the protons at δ 7·16 ppm (H2′), δ 6·98 ppm (H6′) and δ 6·76 ppm (H4) with carbon C2 at 102.3 ppm, characteristic of hemiketal form. The ^{1}H signals of $\mathbf{B_{CD}}$ were found to be downfield shifted with respect to the spectra of **B** before the addition of β-CD. The two epimeric forms could not be distinguishable after complexation, which could be a result of a preferable inclusion of one of the two epimers into β-CD's cavity. Indeed, the use of cyclodextrins for the separation of isomers was already been reported in the literature (Ishizu et al., 2008; Upadhyay & Kumar, 2009). Also, for the protons signals of **Cc** a downfield shifted were observed. Interconversion between *cis*- and *trans*-chalcone is in slow exchange (in the NMR time scale) while the chemical exchange between the hemiketal and the *cis*-chalcone is faster (Pina, 1998; Pina et al., 2012). Bearing this, the chemical shifts changes observed for the *cis*-chalcone could result from the faster chemical exchange. However, based on the NOE interaction observed between this equilibrium form and β-CD and on the alteration of the *D* value, we assume that the chemical shift changes may be a result from the interaction with β-CD's internal protons, namely a steric compression effect (Wood, Hruska, & Saenger, 1977) instead of chemical exchange. Only minor chemical shifts changes were detected in ^{1}H NMR spectra of cy3glc:β-CD for the protons and **Ct** forms.

For the evaluation of the stoichiometry of the inclusion complexes cy3glc:β-CD, Job' continuous variation technique was applied (Job, 1928). For this purpose, solutions with different cy3glc:β-CD molar ratios were prepared and the data were plotted in the form $X_H \Delta\delta$ *versus* X_H, where X_H is the mole fraction of β-CD. The Job's plot showed a maximum at $r = 0.5$ (where $r = [\beta\text{-CD}]/([\beta\text{-CD}] + [\text{Cy3glc}])$), indicating that the complexes possessed a 1:1 stoichiometry.

Moreover, when performing the NMR titration it was noticed that the addition of β-CD affected principally the hydration reaction, mainly disturbing the normalized molar proportions between the flavylium cation and the hydrated hemiketal. The other equilibrium forms, *cis*- and *trans*-chalcones were almost unaffected with the increase of β-CD (Fig. 3A). These preliminary results suggest the preference inclusion of the hemiketal into β-CD with this compound catalyzing the transformation of the flavylium cation into the hemiketal, a phenomenon leading to the shifting of the pigment hydration equilibrium toward the formation of more hemiketal with the addition of more β-CD. The normalized molar proportion of the various equilibrium forms were determined by integration of signals in the ^{1}H NMR spectra. Concurrently, during the same experiments with the addition of β-cyclodextrin a clear change in the color of the anthocyanin solution was observed. β-cyclodextrin induces a strong decrease in the anthocyanin visible absorption band and this decrease was greater with higher concentrations of β-CD added (Fig. 3B). This behavior had already been described in the literature (Dangles, Stoeckel, et al., 1992; Dangles, Wigand, et al., 1992; Fernandes et al., 2013) and suggests a preferential interaction between the anthocyanin hemiketal form and β-CD.

3.3. Diffusion ordered NMR spectroscopy

Diffusion ordered NMR spectroscopy (DOSY) is a well-established technique for characterizing the structure and dynamics of complex systems. The self-diffusion coefficients of these systems reveal structural characteristics such as molecular size, weight and shape (Brand, Cabrita, & Berger, 2005; Cohen, Avram, & Frish, 2005). This methodology relies on the determination of the diffusion coefficients in the absence and presence of host molecules (β-cyclodextrin in this study), thus providing information about the size and evidence on the magnitude of the binding constants (Avram & Cohen, 2002; Fielding, 2000).

Typically, cy3glc is approximately one half of the average size of β-CD. In these DOSY studies it was intended not only in confirming the interactions between cy3glc and β-CD but also distinguishing the affinity of the existing anthocyanin equilibrium species at pD 3.9 for inclusion complex formation with β-CD. Since a modification in a solution composition was expected to induce changes in the behavior of the anthocyanin equilibrium forms, cy3glc:β-CD samples containing cy3glc to β-CD ratio of 1:0.8, 1:1.6, 1:2.4 and 1:3.2 were studied. The diffusion coefficients of β-CD and the existing equilibrium forms of cy3glc in cy3glc:β-CD samples were

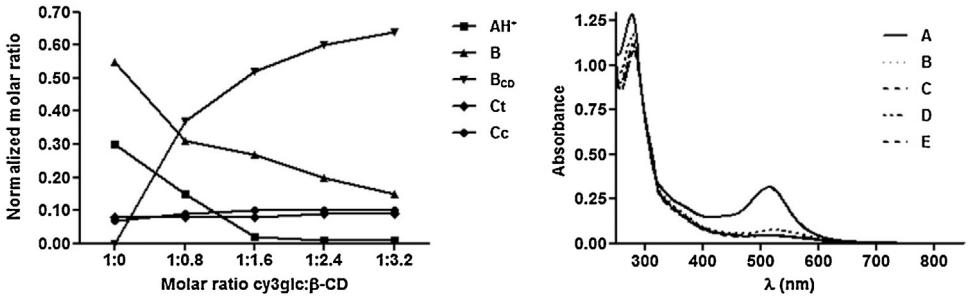

Fig. 3. Normalized molar proportion of the flavylium cation (**AH**$^+$), hemiketal (**B**), *cis*-chalcone (**Cc**), *trans*-chalcone (**Ct**) and hemiketal complexed ($\mathbf{B}_{CD}$) as a function of different β-CD ratios, determined by integration of signals in the ^{1}H NMR spectra (A). UV–visible spectra of cyanidin-3-*O*-glucoside alone and in the presence of β-cyclodextrin at different concentrations (B).

determined and compared with the corresponding values of cy3glc and β-CD alone. The diffusion measurements using DOSY were performed under identical experimental conditions taking special attention on the concentration, pH and temperature of the samples. The diffusion coefficients (*D*) of cy3glc equilibrium forms were obtained by measuring the signal intensity at more than one place in the spectra and those for β-CD from the resonance signals of the anomeric protons. To account for changes in the samples solution viscosity or drift on the experimental conditions, the diffusion coefficient values were all scaled to the absolute *D* value obtained for acetone (0.001 M; 1.69×10^{-9} m^2 s^{-1}, calculated standard deviation of 1.15×10^{-3}) used as an internal reference.

In the absence of β-CD the *D* value of **B**, **Cc** and **Ct** was found to be very similar to 5.5×10^{-10} m^2 s^{-1} (Table 2). The significantly lower *D* value observed for **AH$^+$** was attributed to the tendency of this equilibrium form to self-aggregate resulting on a specie with higher hydrodynamic diameter. Concerning the results obtained for the inclusion complexes cy3glc:β-CD, diverse behavior of the different anthocyanin equilibrium forms in the presence of β-CD was observed. The diffusion coefficients measured for the new set of signals detected in cy3glc:β-CD ($\mathbf{B_{CD}}$) form was found to be similar to the corresponding values of β-CD (4.0×10^{-10} m^2 s^{-1}). This is an indication of intermolecular interactions and complexation between these two species was hence assumed. Likewise, the decrease of the diffusion coefficient of *cis*-chalcone (**Cc**) in cy3glc:β-CD samples, to values close to that of β-CD reveal a possible interaction between these two species. However, only small changes in the self-diffusion of *trans*-chalcone (**Ct**) was observed in the presence of β-CD. This fact and the registered absence of chemical shift displacements of **Ct** resonance signals in the ^{1}H NMR spectra of cy3glc:β-CD strongly suggest a lack of intermolecular interactions between and β-CD.

The flavylium cation diffusion coefficient was almost unchanged and lower than β-CD's during the experiments until the third anthocyanin:β-CD ratio was achieved. At this ratio only traces of the AH$^+$ equilibrium form was detected, not allowing the correct *D* determination (Table 2). The results from the analysis of DOSY spectra of the inclusion complex cy3glc:β-CD indicate that only two of the anthocyanin equilibrium forms, **B** and **Cc**, showed preference for association and affinity for intermolecular complex formation with β-CD. These results are in agreement with the observed chemical shifts alterations registered for protons of **B**, **Cc** and β-CD in ^{1}H NMR spectra of cy3glc:β-CD. The observed changes in the chemical shifts and self-diffusion change for **B** and **Cc** suggest an inclusion of these species into the cavity of β-CD.

Table 2
Diffusion coefficients (*D*) obtained for β-cyclodextrin and for flavylium cation, hemiketal, *cis*-chalcone and *trans*-chalcone equilibrium forms of 1.4 mM cyanidin-3-*O*-glucoside solutions with increasing amounts of β-CD in D_2O at pD 3.9.

Ratio cy3glc:β-CD	$D \times 10^{-10}$ (m^2 s^{-1})				
	AH$^+$	*B*	*Cc*	*Ct*	B_{CD}
1:0.0	4.2	5.4	5.5	5.6	0.0
1:0.8	4.2	5.5	4.0	5.4	3.9
1:1.6	[a]	5.7	3.9	5.5	3.8
1:2.4	[a]	5.8	4.0	5.5	3.8
1:3.2	[a]	5.7	4.0	5.5	3.9

$D_{\beta\text{-CD}} \times 10^{-10}$ (m^2 s^{-1}) = 4.0.
[a] Undetected.

3.4. *Putative structure of the inclusion complex of cy3glc with β-CD*

Beside the chemical shifts changes and changes of diffusion constants initiated by complexation with CD, changes of NOE for the species in the solution serve as a measure of intermolecular binding and inclusion complex formation. Further reliable information on the inclusion complex formation can be obtained by the evaluation of the intermolecular proximity of protons in the guest species to the H3 and H5 protons, located inside of the cyclodextrin cavity by measurements of NOE. Additionally, information can be extracted for the preferred structural arrangement of the guest molecules in the cyclodextrin cavity in the process of inclusion complexes formation.

Therefore, structural investigations based on NOE studies were performed to further determine the behavior and mode of interaction of the different forms of anthocyanin co-existing in aqueous solution at pD 3.9 with β-CD and to define the structure of the cy3glc:β-CD complex. The NOE relies on different correlation times (τ_c) of free and bound molecules and the observation of intermolecular NOE between molecules in solution is a strong indication for intermolecular association processes. Rotating frame nuclear Overhauser spectroscopy (ROESY) was applied to study solutions containing equimolar amounts of β-CD and cy3glc in D_2O. A number of ROESY experiments using a mixing time in the range between 100 and 800 ms were recorded with the aim to discriminate the NOE originating from the bound state of cy3glc with β-CD (intermolecular NOE) and NOE of the non-bounded species in the solution (intramolecular NOE) (Meyer & Peters, 2003). In the ROESY spectrum, the cross-peak connecting two proton resonances indicates that those proton nuclei are in close proximity in the ground state of the molecule (Ishizu et al., 2006). The intensity of the rotating frame nuclear Overhauser effect (ROE) was estimated from the integral volume of the cross-peak and was classified as strong, medium, weak or very weak (Ishizu et al., 2008).

The analysis of 2D ROESY spectra of cy3glc:β-CD acquired at different mixing times showed correlations between protons of cy3glc's hemiketal form complexed with β-CD and H3 and H5 protons lying on the inner surface of β-CD (Fig. 4). The H3 protons of β-CD shares strong intermolecular ROE correlations with protons

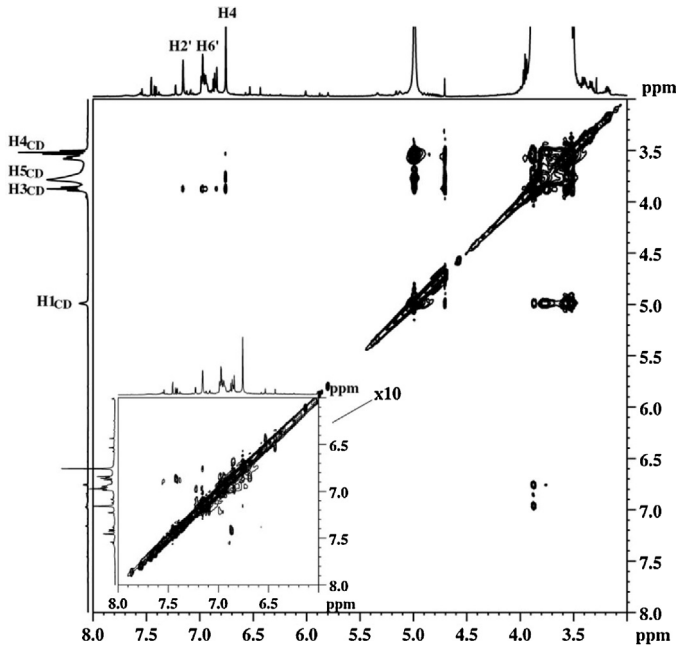

Fig. 4. 2D ROESY (600 MHz) spectra of cy3glc:β-CD (1:1) acquired in D_2O (pD 3.9) with a mixing time of 500 ms, showing characteristic inter- and intra- (expanded spectral area) molecular NOE interactions in the complex. The assignment of resonances of B_{CD} and β-CD is included.

H4 from C-ring and H6′ from ring B, medium intermolecular correlations with proton H2′ and weak intermolecular correlations with proton H5′ (also from B ring) of the hemiketal form **B_{CD}**. H5 of β-CD shares strong ROE correlations with protons H4 (Fig. 4). These observations strongly suggest that the cy3glc's C-ring is deeply included in the β-CD cavity. No NOE interactions were detected between protons from the anthocyanin **B_{CD}** with the outer protons H2 and H4. All together, these data suggest that probably the A- and C-ring are included from the wide secondary hydroxyl group side of the β-CD cavity being closer to the narrow rim, whilst the B-ring lies on the plane of the wider rim of β-CD. This type of molecular inclusion had already been described for other polyphenols, namely for (−)-epicatechin gallate (also presenting a catechol B ring) and (−)-epigallocatechin gallate (presenting a pyrogallol B ring) (Ishizu et al., 2006, 2008).

In this spectrum no dipole–dipole interactions were registered between protons of the flavylium cation and *trans*-chalcone equilibrium forms and β-CD. However, small but detectible NOE was observed between characteristic protons of *cis*-chalcone and β-CD's H3. The structural similarity of the two equilibrium forms **B_{CD}** and **Cc** was assumed to be a reason for their similar behavior in a presence of CD. The presence of a tetrahedral carbon atom in the neutral hemiketal makes it much less rigid then the almost planar flavylium cation and probably allow a closer fit to the macrocyclic cavity. In the *cis*-chalcone the presence of an open chain probably also allows a better molecular inclusion in the hydrophobic cyclodextrin cavity. Additionally, for the charged and highly polar flavylium cation the relative desolvation of the guest molecule when it enters the cyclodextrin cavity is probably more endothermic.

In the 2D ROESY spectra recorded at longer mixing time (500 and 800 ms) weak intramolecular interactions between the anthocyanin protons were observed besides the intermolecular dipole interaction between **B_{CD}** and **Cc** with the interior β-CD cavity protons.

Further details of the solution structure of the complex were obtained from Molecular Dynamics simulation.

Table 3
Distance values obtained for the closest contacts between the hydrogen atoms of cy3glc and β-CD compounds.

Atom of cy3glc	Atom of β-CD	Distance (Å)
H4	H3-Glc7 and H_5-Glc7	3.29 ± 1.02 and 3.22 ± 0.82
H6	–	–
H8	H3-Glc3 and H_5-Glc3	3.60 ± 1.24 and 2.93 ± 0.93
H2′	H3-Glc5	4.87 ± 1.47
H5′	H3-Glc5	4.66 ± 1.77
H6′	H3-Glc5	4.56 ± 1.65

3.5. Structure of the inclusion complex cy3glc-β-CD by Molecular Dynamics simulation studies

To better understand the inclusion of the hemiketal cy3glc form in the hydrophobic β-CD's internal cavity, computational studies were additionally carried out. An MD simulation of 30 ns was performed for this complex, which allowed the respective conformational space to be sampled. The last 20 ns of this MD simulation were used for the subsequent structural analysis. The root–mean–square deviation (RMSD) value obtained for this compound was 2.92 ± 0.62 Å. This small value reveals higher equilibration and stability of this complex during the MD simulation. Fig. 5 shows the closest structure to the average geometry of cy3glc-β-CD complex, which is in good agreement with the data obtained in the NMR studies. In order to measure the movement of the cy3glc molecule relative to the average structure over the whole simulation, root–mean–square fluctuation (RMSF) values by atom were also calculated. Analysing these values it was noticed higher RMSF values for the main hydroxyl groups of the glucose unit and the HO-C3′ group of the B ring, as well as for the H5′ and H6′ atoms which reveal a higher degree of flexibility during the MD simulation. The dynamic behavior of these atoms agrees with their previously referred close contact with solvent molecules.

To clarify the binding and inclusion mode of cy3glc:β-CD complex, the distances between all H atoms of A-, B- and C-rings of the hemiketal and the H1, H2, H3, H4 and H5 atoms of each glucose unit from the β-CD were also calculated during the MD simulation. Table 3 shows the average distances of the closest contacts between the hydrogen atoms of cy3glc and the β-CD molecules. As seen in the Molecular Dynamics simulation, the binding and inclusion of cy3glc in the cavity of β-CD are ensured by the establishment of hydrophobic interactions between the polyphenolic and glucose rings, as well as hydrogen bonds with the hydrophilic hydroxyl polar groups of both compounds. All these crucial interactions contribute to the formation and stabilization of this complex. As seen in Fig. 5, the A- and C-nucleus of cy3glc provide the major contribution to the binding driving force, followed by the B-ring, whilst its glucose residue seems to perturb the cy3glc's inclusion in the β-CD and is facing the solvent. Similarly to the present NMR studies, these results also reveal a higher proximity between the H4, H2′, H5′ and H6′ atoms of cy3glc and the internal H3 and H5 atoms of several glucose units, in particular the Glc3, Glc5 and Glc7 units. It was also obtained large distances to the outer H1, H2 and H4 atoms of β-CD, and it is noteworthy that the H6 at the A-ring of cy3glc is very distant to the hydrogen atoms of β-CD and directed to the solvent molecules during the whole simulation (data not shown). To better characterize this cy3glc:β-CD inclusion mode, the solvent-accessible surface area (SASA) values for some nonpolar H atoms of both cy3glc (H4, H6, H8, H2′, H5′ and H6′) and β-CD (H1, H2, H3, H4 and H5) molecules during the MD simulation were calculated. The SASA defines the surface area of a group/atom that is accessible to a solvent probe and indicates which atoms are most exposed to the solvent. Table 4 shows the obtained SASA values with standard deviations for each atom. As expected, the outer H1, H2 and H4 atoms of β-CD have shown higher values. On the other hand, the

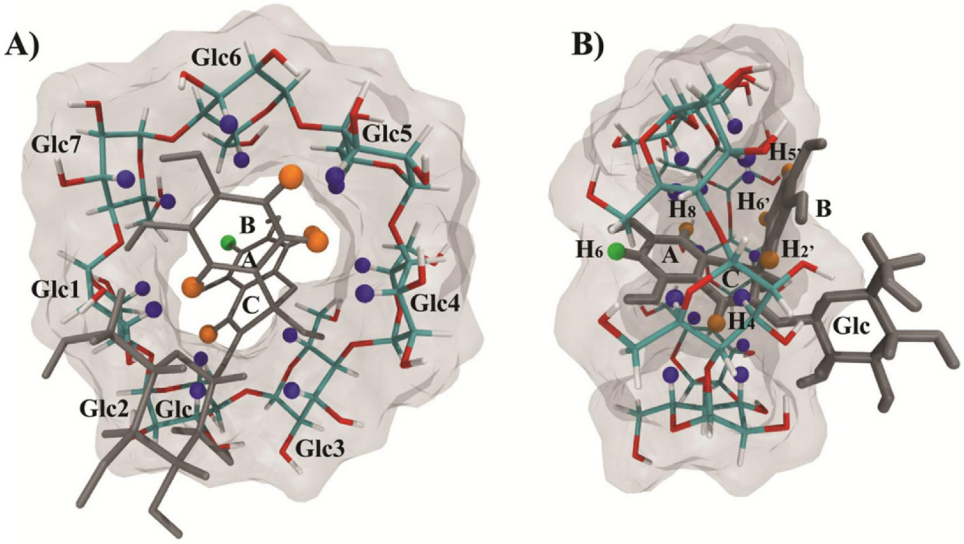

Fig. 5. Structure of cy3glc:β-CD complex in front-view (A) and side-view (B). The β-CD is represented with surface and colored by atom type, the cy3glc is represented with sticks and colored in gray. All H3 and H5 protons of each glucose unit from β-CD are colored in blue, while the nonpolar hydrogen atoms from the cy3glc are colored in orange (H4, H8, H2′, H5′ and H6′) and green (H6).

Table 4
SASA values obtained for several hydrogen atoms of cy3glc and β-CD molecules.

Atom	SASA (Å^2)
H1-Glc of β-CD	74.55 ± 4.89
H2-Glc of β-CD	108.42 ± 3.85
H3-Glc of β-CD	2.03 ± 3.37
H4-Glc of β-CD	44.90 ± 3.98
H5-Glc of β-CD	0.20 ± 0.56
H4 of cy3glc	0.03 ± 0.32
H6 of cy3glc	7.82 ± 2.83
H8 of cy3glc	0.05 ± 0.28
H2′ of cy3glc	2.26 ± 2.63
H5′ of cy3glc	5.34 ± 3.43
H6′ of cy3glc	2.61 ± 3.54

internal H3 and H5 atoms present smaller values of SASA, which agrees with the hydrophobic environment of β-CD's cavity. Relatively to the cy3glc molecule, the higher SASA value was obtained for the H6 atom (7.82 ± 2.83 Å^2), which indicates that this specific atom is highly exposed to the solvent. On the other hand, minimal SASA values were obtained for H4, H8, H2′, H5′ and H6′. According to the SASA values obtained, a higher protection of H4, H8, H2′, H5′ and H6′ atoms was noticed due to the interaction with the β-CD molecule. Therefore, the hydrophilic environment around the H6 of cy3glc point out by this data demonstrates that this atom is proximal to solvent water molecules and is directed to the exterior of the β-CD cavity.

4. Conclusion

Nuclear Magnetic Resonance analysis and Molecular Dynamics simulation performed in this study have clearly proved the selective inclusion of the anthocyanin hemiketal form into the β-CD cavity. This assumption was based on the anthocyanin chemical shift alteration after complexation with β-CD, decrease on the diffusion coefficient of the hemiketal equilibrium form to values close to the corresponding values of β-CD and on the observed NOE effect between this equilibrium form with CD's interior protons. The computational data support and clarify the successful inclusion of the cy3glc molecule inside the hydrophobic cavity of β-CD proposed by the present experimental studies.

The results achieved offer a contribution to the elucidation of the formation and the structure of inclusion complexes between the equilibrium network of anthocyanins forms and cyclodextrins increasing the knowledge regarding the phenomena that drive the stabilization of these natural colorants.

Acknowledgments

This work received financial support from FEDER funds through COMPETE, POPH/FSE, QREN and FCT (Fundação para a Ciência e Tecnologia) from Portugal by one PhD scholarship (SFRH/BD/65350/2009) and through projects PTDC/QUI/67915/2006, PTDC/QUI/122916/2010 and PEst-C/QUI/UI0081/2011. The Bruker Avance III 600 HD spectrometer was purchased under the framework of QREN, through project NORTE-07-0162-FEDER-000048, and is part of the Portuguese NMR Network created with support of the Portuguese Foundation for Science and Technology through contract REDE/1517/RMN/2005, with funds from POCI 2010 (FEDER) and (FCT). To all financing sources the authors are greatly indebted.

Appendix A. Supplementary data

Supplementary data associated with this article can be found, in the online version, at http://dx.doi.org/10.1016/j.carbpol.2013.11.037.

References

Avram, L., & Cohen, Y. (2002). Complexation in pseudorotaxanes based on α-cyclodextrin and different α,ω-diaminoalkanes by NMR diffusion measurements. *Journal of Organic Chemistry*, *67*(8), 2639–2644.

Azevedo, J., Fernandes, I., Faria, A., Oliveira, J., Fernandes, A., de Freitas, V., et al. (2010). Antioxidant properties of anthocyanidins, anthocyanidin-3-glucosides and respective portisins. *Food Chemistry*, *119*(2), 518–523.

Basma, M., Sundara, S., Calgan, D., Vernali, T., & Woods, R. J. (2001). Solvated ensemble averaging in the calculation of partial atomic charges. *Journal of Computational Chemistry*, *22*(11), 1125–1137.

Bayly, C. I., Cieplak, P., Cornell, W. D., & Kollman, P. A. (1993). A well-behaved electrostatic potential based method using charge restraints for deriving atomic charges – The resp model. *Journal of Physical Chemistry*, *97*(40), 10269–10280.

Bourvellec, C. (2003). *Association entre les procyanidols et les polymères pariétaux de pommes: quantification et conséquences*. Universite de Rennes I: (Vol. Docteur).

Brand, T., Cabrita, E. J., & Berger, S. (2005). Intermolecular interaction as investigated by NOE and diffusion studies. *Progress in Nuclear Magnetic Resonance Spectroscopy*, *46*(4), 159–196.
Brouillard, R., & Delaporte, B. (1977). Chemistry of anthocyanin pigments. 2. Kinetic and thermodynamic study of proton transfer, hydration, and tautomeric reactions of malvidin 3-glucoside. *Journal of the American Chemical Society*, *99*(26), 8461–8468.
Brouillard, R., & Dubois, J. E. (1977). Mechanism of the structural transformations of anthocyanins in acidic media. *Journal of the American Chemical Society*, *99*(5), 1359–1364.
Brouillard, R., & Lang, J. (1990). The hemiacetal-cis-chalcone equilibrium of malvin, a natural anthocyanin. *Canadian Journal of Chemistry*, *68*, 755.
Cala, O., Dufourc, E. J., Fouquet, E., Manigand, C., Laguerre, M., & Pianet, I. (2012). The colloidal state of tannins impacts the nature of their interaction with proteins: The case of salivary proline-rich protein/procyanidins binding. *Langmuir*, *28*(50), 17410–17418.
Case, D. A., Darden, T. A., Cheatham, I. T. E., Simmerling, C. L., Wang, J., Duke, R. E., et al. (2008). *AMBER 10*. San Francisco: University of California.
Chandra, A., Nair, M. G., & Iezzoni, A. F. (1993). Isolation and stabilization of anthocyanins from tart cherries (*Prunus cerasus* L.). *Journal of Agricultural and Food Chemistry*, *41*(7), 1062–1065.
Clifford, M. N. (2000). Anthocyanins – Nature, occurrence and dietary burden. *Journal of the Science of Food and Agriculture*, *80*(7), 1063–1072.
Cohen, Y., Avram, L., & Frish, L. (2005). Diffusion NMR spectroscopy in supramolecular and combinatorial chemistry: An old parameter—New Insights. *Angewandte Chemie International Edition*, *44*(4), 520–554.
Dangles, O., Stoeckel, C., Wigand, M. C., & Brouillard, R. (1992). Two very distinct types of anthocyanin complexation: Copigmentation and inclusion. *Tetrahedron Letters*, *33*(36), 5227–5230.
Dangles, O., Wigand, M. C., & Brouillard, R. (1992). Anthocyanin anti-copigment effect. *Phytochemistry*, *31*(11), 3811–3812.
Del Valle, E. M. M. (2004). Cyclodextrins and their uses: A review. *Process Biochemistry*, *39*(9), 1033–1046.
Ersus, S., & Yurdagel, U. (2007). Microencapsulation of anthocyanin pigments of black carrot (*Daucuscarota* L.) by spray drier. *Journal of Food Engineering*, *80*(3), 805–812.
Essmann, U., Perera, L., Berkowitz, M. L., Darden, T., Lee, H., & Pedersen, L. G. (1995). A smooth particle mesh Ewald method. *Journal of Chemical Physics*, *103*(19), 8577–8593.
Fernandes, A., Sousa, A., Azevedo, J., Mateus, N., & de Freitas, V. (2013). Effect of cyclodextrins on the thermodynamic and kinetic properties of cyanidin-3-*O*-glucoside. *Food Research International*, *51*(2), 748–755.
Fielding, L. (2000). Determination of association constants (K_a) from solution NMR data. *Tetrahedron*, *56*, 6151–6170.
Frisch, M. J., Trucks, G. W., Schlegel, H. B., Scuseria, G. E., Robb, M. A., Cheeseman, J. R., et al. (2009). *Gaussian 09*.
Gaussian Inc., C.O. P., Bldg. 6, Pittsburgh, PA 15106, USA.
He, J. A., & Giusti, M. M. (2010). Anthocyanins: Natural colorants with health-promoting properties. In M. P. Doyle, & T. R. Klaenhammer (Eds.), *Annual review of food science and technology* (Vol. 1) (pp. 163–187). Palo Alto: Annual Reviews.
Hoshino, T., Matsumoto, U., Harada, N., & Goto, T. (1982). Evidence for the self-association of anthocyanins IV. PMR spectroscopic evidence for the vertical stacking of anthocyanin molecules. *Tetrahedron Letters*, *23*(4), 433–436.
Houbiers, C., Lima, J. C., Maçanita, A. L., & Santos, H. (1998). Color stabilization of malvidin 3-glucoside: Self-aggregation of the flavylium cation and copigmentation with the *Z*-chalcone form. *Journal of Physical Chemistry B*, *102*(18), 3578–3585.
Howard, L. R., Brownmiller, C., Prior, R. L., & Mauromoustakos, A. (2013). Improved stability of chokeberry juice anthocyanins by β-cyclodextrin addition and refrigeration. *Journal of Agricultural and Food Chemistry*, *61*(3), 693–699.
Hwang, T. L., & Shaka, A. J. (1995). Water suppression that works. Excitation sculpting using arbitrary wave-forms and pulsed-field gradients. *Journal of Magnetic Resonance, Series A*, *112*(2), 275–279.
Ishizu, T., Hirata, C., Yamamoto, H., & Harano, K. (2006). Structure and intramolecular flexibility of β-cyclodextrin complex with (−)-epigallocatechin gallate in aqueous solvent. *Magnetic Resonance in Chemistry*, *44*(8), 776–783.
Ishizu, T., Kajitani, S., Tsutsumi, H., Yamamoto, H., & Harano, K. (2008). Diastereomeric difference of inclusion modes between (−)-epicatechin gallate, (−)-epigallocatechin gallate and (+)-gallocatechin gallate, with β-cyclodextrin in aqueous solvent. *Magnetic Resonance in Chemistry*, *46*(5), 448–456.
Izaguirre, J. A., Catarello, D. P., Wozniak, J. M., & Skeel, R. D. (2001). Langevin stabilization of molecular dynamics. *Journal of Chemical Physics*, *114*(5), 2090–2098.
Job, P. (1928). Formation and stability of inorganic complexes in solution. *Annali di Chimica*, *9*, 113–203.
Jordheim, M., Fossen, T., & Andersen, Ø. M. (2006). Characterization of hemiacetal forms of anthocyanidin 3-*O*-β-glycopyranosides. *Journal of Agricultural and Food Chemistry*, *54*(25), 9340–9346.
Kirschner, K. N., & Woods, R. J. (2001a). Quantum mechanical study of the nonbonded forces in water–methanol complexes. *Journal of Physical Chemistry A*, *105*(16), 4150–4155.
Kirschner, K. N., & Woods, R. J. (2001b). Solvent interactions determine carbohydrate conformation. *Proceedings of the National Academy of Sciences of the United States of America*, *98*(19), 10541–10545.
Lewis, C. E., Walker, J. R. L., & Lancaster, J. E. (1995). Effect of polysaccharides on the colour of anthocyanins. *Food Chemistry*, *54*(3), 315–319.
Leydet, Y., Gavara, R., Petrov, V., Diniz, A. M., Parola, A. J., Lima, J. C., et al. (2012). The effect of self-aggregation on the determination of the kinetic and thermodynamic constants of the network of chemical reactions in 3-glucoside anthocyanins. *Phytochemistry*, *83*, 125–135.
Matsumoto, N., Yamada, M., Kurakata, Y., Yoshida, H., Kamitori, S., Nishikawa, A., et al. (2009). Crystal structures of open and closed forms of cyclo/maltodextrin-binding protein. *FEBS Journal*, *276*(11), 3008–3019.
Meyer, B., & Peters, T. (2003). NMR spectroscopy techniques for screening and identifying ligand binding to protein receptors. *Angewandte Chemie International Edition*, *42*(8), 864–890.
Mourtzinos, I., Makris, D. P., Yannakopoulou, K., Kalogeropoulos, N., Michali, I., & Karathanos, V. T. (2008). Thermal stability of anthocyanin extract of *Hibiscus sabdariffa* L. in the presence of β-cyclodextrin. *Journal of Agricultural and Food Chemistry*, *56*(21), 10303–10310.
Pianet, I., André, Y., Ducasse, M. A., Tarascou, I., Lartigue, J. C., Pinaud, N., et al. (2008). Modeling procyanidin self-association processes and understanding their micellar organization: A study by diffusion NMR and molecular mechanics. *Langmuir*, *24*(19), 11027–11035.
Pina, F. (1998). Thermodynamics and kinetics of flavylium salts. Malvidin revisited. *Journal of the Chemical Society, Faraday Transactions*, *94*(15), 2109–2116.
Pina, F., Melo, M. J., Laia, C. A. T., Parola, A. J., & Lima, J. C. (2012). Chemistry and applications of flavylium compounds: A handful of colours. *Chemical Society Reviews*, *41*(2), 869–908.
Polyakov, N. E., Leshina, T. V., Hand, E. O., Petrenko, A., & Kispert, L. D. (2004). β-Ionone cyclodextrins inclusion complexes: ^{1}H NMR study and photolysis. *Journal of Photochemistry and Photobiology A: Chemistry*, *161*(2/3), 261–267.
Popov, K., Rönkkömäki, H., & Lajunen, L. H. J. (2006). Guidelines for NMR measurements for determination of high and low pK_a values (IUPAC Technical Report). *Pure and Applied Chemistry*, *78*(3), 663–675.
Ryckaert, J. P., Ciccotti, G., & Berendsen, H. J. C. (1977). Numerical-integration of cartesian equations of motion of a system with constraints – Molecular-dynamics of N-alkanes. *Journal of Computational Physics*, *23*(3), 327–341.
Rymdén, R., Carlfors, J., & Stilbs, P. (1983). Substrate binding to cyclodextrins in aqueous solution: A multicomponent self-diffusion study. *Journal of inclusion phenomena*, *1*(2), 159–167.
Santos, H., Turner, D. L., Lima, J. C., Figueiredo, P., Pina, F. S., & Maçanita, A. L. (1993). Elucidation of the multiple equilibria of malvin in aqueous solution by one- and two-dimensional NMR. *Phytochemistry*, *33*(5), 1227–1232.
Szejtli, J. (2003). Cyclodextrins. In P. Tomasik (Ed.), *Chemical and functional properties of food saccharides*. Cracow: CRC Press.
Tamura, H., Takada, M., et al. (1998). The Color Stability and Antioxidative Activity of an Anthocyanin and b-Cyclodextrin Complex. *Functional Foods for Disease Prevention I*, *701*, 157–171.
Thaning, J., Stevensson, B., Ostervall, J., Naidoo, K. J., Widmalm, G., & Maliniak, A. (2008). NMR studies of molecular conformations in α-cyclodextrin. *Journal of Physical Chemistry B*, *112*(29), 8434–8436.
Torskangerpoll, K., & Andersen, Ø. M. (2005). Colour stability of anthocyanins in aqueous solutions at various pH values. *Food Chemistry*, *89*(3), 427–440.
Upadhyay, S. K., & Kumar, G. (2009). NMR and molecular modelling studies on the interaction of fluconazole with β-cyclodextrin. *Chemistry Central Journal*, *3*, 9.
Wood, D. J., Hruska, F. E., & Saenger, W. (1977). Proton NMR study of the inclusion of aromatic molecules in α-cyclodextrin. *Journal of the American Chemical Society*, *99*(6), 1735–1740.
Wu, D. H., Chen, A. D., & Johnson, C. S. (1995). An improved diffusion-ordered spectroscopy experiment incorporating bipolar-gradient pulses. *Journal of Magnetic Resonance, Series A*, *115*(2), 260–264.
Yamada, T., Komiya, T., & Akaki, M. (1980). Formation of an inclusion complex of anthocyanin with cyclodextrin. *Agricultural and Biological Chemistry*, *44*(6), 1411–1413.